Keyan Rahimzadeh, Evan Levelle, John Douglas

Beyond the Hypar: Predicting Buckled Shapes in Bent Glass with Machine Learning

Abstract: The cold-bending of rectangular glass panels into anticlastic shapes is a well-established practice. A recently built project consists of four towers featuring thousands of individually unique glass panels which are non-rectangular, cold-bent to an extreme degree, and sometimes curved. The depth of bending in the panels approaches the elastic instability limit, which prompts several challenges: 1) edges no longer remain linear, thereby becoming incompatible with linear frames, 2) surfaces produced by CAD packages do not account for secondary nonlinear effects, and therefore are not accurate enough to fabricate, 3) some panels combine curving and bending, which, along with the parallelogram shape, place the problem outside the bulk of related literature which uses flat, rectangular shapes as a basis. To enable fabrication within an accelerated timeline, a Machine Learning model was trained on 3,500 material simulations that are parametrically generated from the Building Information Model. The model was then deployed to predict the 3-dimensional surface of each unique panel while accounting for non-linear effects, and ensuring straight, linear edges after deformation. The paper describes the geometric problem, including how buckling effects manifest differently in non-rectangular shapes; the development and deployment of the Machine Learning model; and comparisons to physical specimens, including the final construction of some 11,000 unique panels.

1 Introduction

In the pursuit of realizing architectural projects with free-form geometries, the technique of cold-bending glass has seen growing adoption. Among the many challenges that the technique presents is the intractability of predicting the surface geometry that the glass will have after its deformation.

As we discuss in detail, the further you bend the glass, the more the real-world surfaces of glass diverge from the theoretical surfaces created in CAD packages. Predicting the final geometry is useful for many reasons, such as understanding visual reflections. Here we tackle the challenge of reverse-engineering the flat shape of these warped panels, such that they can be fabricated accurately.

There is an ever-growing body of research regarding cold-bent glass; the work presented here has a unique mix of characteristics:

- The panels are quadrilaterals but highly non-rectangular.
- The depth of bending is substantial enough to approach the elastic buckling limit, thereby exhibiting nonlinear behavior.

https://doi.org/10.1515/9783111162683-011

- Every single panel is different, therefore requiring an approach for solving the geometry of each one.
- Techniques were needed that were consistent and compatible with contemporary engineering practice (e. g. Finite Element Analysis), and could be verified.

2 Background and Methodology

2.1 Project Description

The project motivating this research consists of four high rise towers located in Qatar. The facades have a 50/50 mix of vision and opaque panels. Each building can be represented as a morph between two different curved shapes, with a spiraling subdivision pattern; each panel takes the shape of a parallelogram that is non-planar and unique.

The schedule was compressed, moving from architectural concept to first fabricated panel in less than two years, with 23,000 panels fabricated and installed within another two years.

Fig. 1: Construction Project

2.2 Methodology

The research detailed herein was carried out in the process of executing a construction project, and therefore subject to constraints of schedule, cost, and the need to be implemented immediately, and at scale. The investigation and the solution had to be developed simultaneously, an approach commonly called “action research”.

We drew upon our practical knowledge of the literature available and the state of the art, and prioritized development that we knew could be implemented with a predictable – and short – timeline, with a reliable degree of quality. We therefore favored an approach grounded in methods that were familiar to the industry (e. g. finite

elements, parametric modeling, etc.), and could be easily interpreted or even replicated by 3rd party reviewers.

2.3 Facade System

The buildings contain 11,716 glazed panels with bending depths ranging from 10mm to 442 mm. Some panels also needed to be curved at the top edge, bottom edge, or both, to avoid clashes with the slab. Panels with less than 180 mm[1] of deformation are fabricated flat and deformed out of plane when they are mounted to the frame, which were assembled in their final 3-dimensional shape after being fabricated digitally. The development of the 3D framing is discussed in detail by the authors in a forthcoming publication.

For all panels that were curved and/or above the 180 mm threshold, the glass is produced using a different method: both layers of the IGU are made of laminated glass. The glass is deformed out of plane in the factory before going into the autoclave and being laminated "in-place". Once laminated, the structural interlayer' stiffness helps retain the deformed shape. This is sometimes called "Lamination Bending"[2] or "Warm Bending"; we include it here within the "Cold Bending" category as the process never raises the temperature enough to alter the properties of the glass itself.

3 Geometry of Cold Bent Surfaces

Design of cold-bent glazing must consider a range of technical concerns regarding structural mechanics, engineering, and system design (Datsiou 2017, Beer 2015, Nardini 2018). Here we focus on the geometric aspects of the problem.

It is a known phenomenon that as glass is deformed elastically out of plane, a secondary mode emerges that diverges from the idealized shape of a hyperbolic paraboloid (Bensend 2015, 2016). While a hyperbolic paraboloid is a double-ruled surface, it is anticlastic and not developable; it follows therefore that glass, being rigid, cannot be forced into such a shape.

It is also established that above a certain level of distortion, "linear Kirchhoff–Love theory of plates [does not apply, so] the plate bulges into an asymmetric configuration and the edges are not any more straight" (Galuppi 2014). In this project, we found that the panels' edges deviated from in-plane straightness by as much as 6.5 mm. This

1 This threshold is derived in more detail in later sections.

2 This technique is known to exhibit behavior wherein the final shape "varies in time due to the viscosity of the polymeric interlayer" (Galuppi 2015). The panels in this project however are adhered to a rigid structural frame, and the long edges further have an exterior cap, which together work to retain the perimeter shape of the panel.

is consistent with in-plane edge deviations found in other studies (Eversmann et al. 2016). Other related work also indicates that optimal shape finding must "reduce the tangential force exerted at the boundary" (Gavriil et al. 2020).

The suggestion is that edges should not be assumed straight on the fabricated shape; rather, to develop a methodology that accounts for the distortions such that panels have straight edges *when in their final position.* This is important because the vertical framing elements are also straight; any deviation in the glass edge straightness could compromise the quality of the structural bond between the glass and the frame (Fig. 2). Through discussions with the fabricator, we set a target deviation of 1.0 mm.

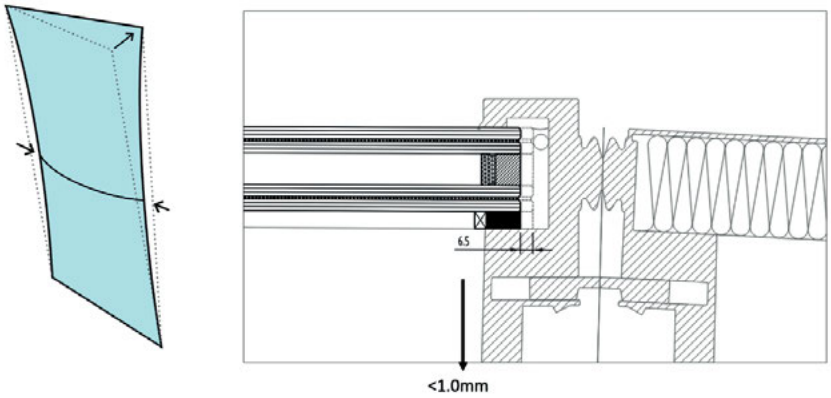

Fig. 2: As the edge deviates from straight, it affects the structural interface with the frame.

Some existing work puts an emphasis on pursuing shapes that conform to architectural design surfaces (Gavriil et al. 2020, Beer 2015) or an assessment of "cold bending distortion… and the resulting optical quality" (Datsiou 2016), but here priority is given to the geometrical conformance between panel edges and the framing.

3.1 Effects of Non-Rectangularity

As mentioned above, the bulk of existing literature assumes panels that are rectangular. Rectangles alone cannot tile most complex surfaces. As the shape deviates from rectangular, the buckling behavior of glass panels changes. We include here a parametric study of panels with skewed, parallelogram shapes, in line with the panels of the project. The study indicates that between 50 mm and 100 mm of skew, there is a bifurcation in behavior in the buckling behavior (Fig. 3).

Bensend establishes a non-dimensional twist ratio, denoted k, and suggests that for rectangular panels the moment of buckling usually begins when $k = 13.5$. The

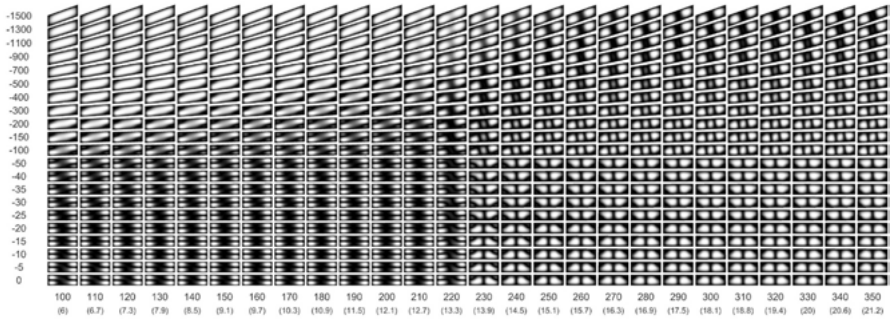

Fig. 3: Plot of surface deviations relative to idealized hypar surface. Above image shows plots normalized to the maximum of each individual panel. Below image is normalized to the maximum across all samples. The horizontal axis shows depth of bending in real dimensions and non-dimensional *k*-factor (in parentheses).

parametric study above indicates a bifurcation in buckling behavior between k_{buckling} values of 13.3 and 13.9, which is consistent. Plots below show that as the skew increases, the deviation from a hypar is greater, even at small amounts of bending. As bending approaches the buckling limit, rectangular panels show a sharp increase in shape changes, while the skewed panels have a more subtle transition (Fig. 4 and Fig. 5).

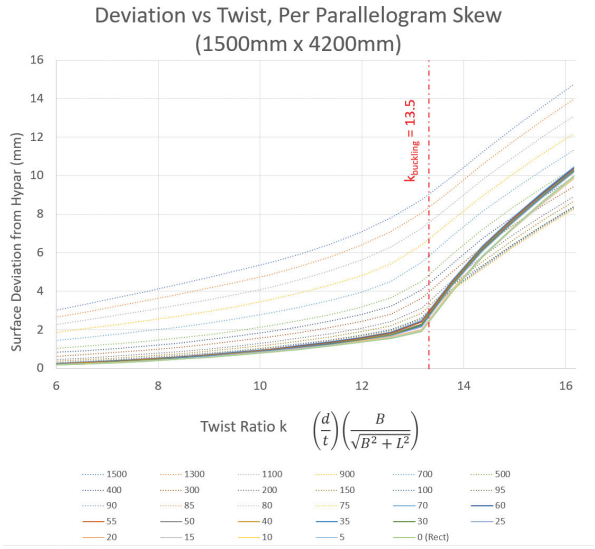

Fig. 4: Comparison of surface deviation and panel twist for different dimensions of panel skew.

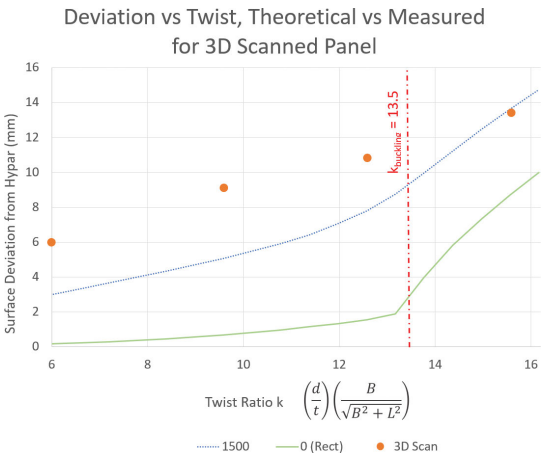

Fig. 5: Surface deviation vs panel twist for 3D Scanned panel, compared to theoretical for skewed and rectangular equivalent.

3.2 Preliminary Physical Testing

Prototype panels were fabricated, with 3D scans performed for comparison with the structural simulations from Finite Element Analysis (FEA) and deviations from the theoretical surfaces. The prototypes clearly exhibited the secondary nonlinear effects consistent with the FEA, though the results are not a perfect match. While broadly consistent, with two local "bulges" of deviation, there are distinct ripples in the pattern (Fig. 6). These are artifacts from the plastic bag draped across the back of the glass, the shadows of which may affect the registration of the scanner. The scanning results were only available after the prototype testing had concluded, and the timeline did not allow for further testing. In future studies, it would be preferable to mask the panel with tape or otherwise opaque material.

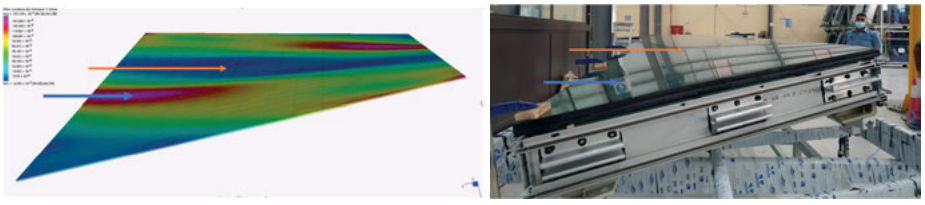

Fig. 6: Correlation of FEA simulations and fabricated panels.

Having built, bent, and scanned multiple prototypes, the scans were post-processed to measure the point clouds against the theoretical hyperbolic paraboloid, for different degrees of bending/twist. Due to the inherent noise in the sampling, as well as errant

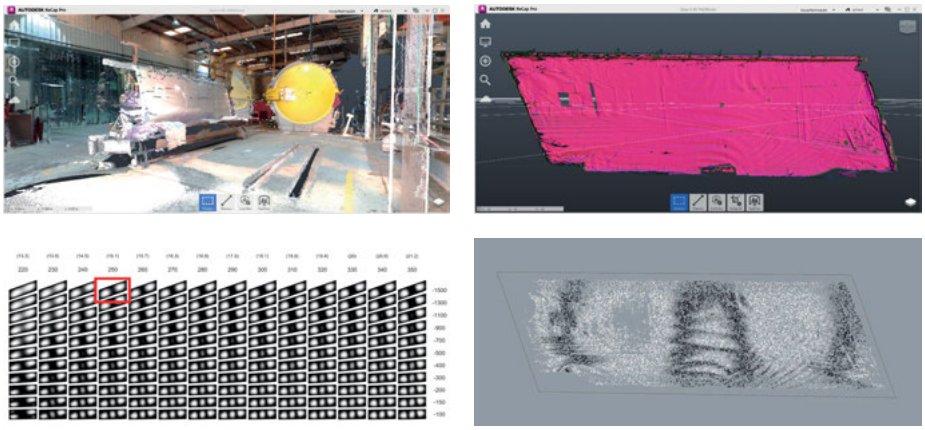

Fig. 7: Top left: color view of full 3D scan; top right: selected area of 3D scan, indicating normals as measured by scanner; bottom right: calculated deviation of 3D scan from theoretical surface; bottom left: corresponding plot of expected deviation according to FEA.

scan points due to things like clamps and other hardware, statistically distinct outliers were removed from the data.

As the panel approaches and passes the buckling limit, the scans converge with the expected simulation results. Below this level, the scans show greater deviation from the theoretical than we would expect from the FE analysis. We believe this is due to the realities of fabrication and construction, for example imperfect boundary conditions: FEA can represent infinitely stiff edge conditions, while in reality, materials flex and bend, and the restraints on the panel will have some additional give, thereby introducing greater deviations.

While a tighter match between the FEA and the scans would be preferred, the overall buckled shape of the glass was consistent with our simulations (Fig. 6), and the further the panel was bent, the tighter the numerical correlation.

Bensend suggests a knock down factor of 0.6 to the twist factor if buckling is to be all together avoided. This sets the threshold at 180 mm as discussed previously. When accounting for the thinner plies used in the lamination bending, that 180 mm threshold is equivalent to a k-factor of 10.8, as shown in Fig. 4. Further confidence is provided because the correlation between scans and simulations are stronger above this level.

4 Machine Learning

To accurately unroll the glass surface, one must accurately predict the 3-dimensional surface, accounting for the material properties and nonlinear buckling effects de-

scribed in the previous section. For this project we chose to pursue a Machine Learning (ML) approach with integrated Finite Element Analysis. Listed below are the primary considerations that influenced this decision.

1. *Inputs are highly interdependent*. The shape of the panel is defined by several parameters. To determine the relative influence of these inputs, one must perform many simulations and/or tests and perform a sensitivity analysis. One strength of ML algorithms is that the interaction of inputs is computed as part of the regression process – they do not have to be known in advance.
2. *Requirement for a large set of simulations.* Any analytical technique would require simulations or tests for validation. If the large dataset is required regardless of the technique, then opting for a ML model sidesteps the need for heavy analytical work, instead using analysis for intermittent checks to ensure the model outputs are reasonable.
3. *Integration with industry standard workflows*. Ultimately a mathematical description of the surface would need to be translated into a CAD package. Previous work that aims to predict glass panel outcomes from definition of its shape is primarily aimed at providing singular numerical values that are relevant to the engineer, such as peak deflection or peak stress. The more sophisticated of those techniques rely on a large array of tabulated data along that would require the practitioner to do several interpolations (Galuppi 2020). We instead pursued an approach that could exist "natively" inside of our 3D modeling environment.
   The process we deployed generates simulations directly from the model, trains the ML model, and returns data points in a model-friendly format (this is expanded upon below). This avoids having to translate data between different contexts (e. g. CAD to mathematical formulations and back), and leverages the tried and tested surfacing algorithms in the 3D CAD environment for representation. Being able to use verified, trusted FEA packages also gave us greater confidence in the approach, because each database entry could be retrieved, opened, interrogated, or even shared with other engineers. Strand7 was used for our simulations, which is an industry standard package, such that most 3rd party reviewers would be able to review or even replicate any simulation in a software package that they know and trust.
4. *Flexibility and Generalization*. The ML model employed here simply analyzed three parameters (described below), whereas the largest machine learning models in use today have tens of billions of parameters, so the principles of this approach could be used to encompass a more general set of panel geometries.

4.1 Automated Generation of FEA models

To produce a ML model, one must first compile the data on which the model is trained. Since it is important that the database accounts for the physical behavior of the plates,

the database is comprised of structural simulations that encompass the range of panel geometries in the project.

To establish the training set, each panel starts as a NURBS surface from Rhino that generates a quad mesh that is suitable for FEA. The twisted surface is then "pulled flat" in a simulation process that constrains its edges to the ground plane, allowing the center of the panel to deform and buckle as necessary within that flat boundary. The aim in this step is to approximate what the final flat shape might be. The perimeter of the "flattened" panel is then extracted, and a new mesh, truly flat, is created from it. That new mesh is then pushed back to 3D, again with edges constrained. This simulated shape will now feature the characteristic "bulges" as indicated in the prototypes.

4.2 Shape Functions and Parameterization

When designing a ML model, one of the most important decisions is the selection of inputs and outputs. For this study, inputs are selected to provide a numerical representation of the panel perimeter, and outputs constitute a numerical representation of the surface.

For the inputs, the panel perimeter is known in advance. The known parameters that vary from panel-to-panel include: Out-of-plane bending dimension, top edge curvature, bottom edge curvature, internal angles of the parallelogram, top edge length, and bottom edge length. For the outputs, we needed to define discrete numerical values that can define a continuous surface. To do this, we borrowed a concept from Finite Element methods called a Shape Function. In FEA, this is a function that allows for computation of a value within the field of an element, based on the values at its nodes.

A similar approach is used in Galuppi (2020) to determine peak stress or deflection, where ours is for recreating surface geometry. We selected 7 locations within the field of the quadrilateral, and measured their deviation from the idealized CAD geometry. The locations were selected by a process of trial and error but followed an underlying logic: if/when the top and bottom edges of the panel are curved, three points provide sufficient definition of the resulting nearby curvature (P1–P3 for the top, P5–P7 for the bottom).

We determined that the panel's central area could be defined with a single sample point – the curvature across the center was always symmetrical and sufficiently described by a single interpolation point. Through development of the mapping functions, we also found that some input parameters had weak correlations, and could be ignored. For example, the internal angle of the panel appears to have very little correlation with sample point P3, whereas the depth of bending has a clear correlative relationship (Fig. 8).

After analysis, the only three inputs required were the first three listed above: depth of bending, and curvature of the top and bottom edges.

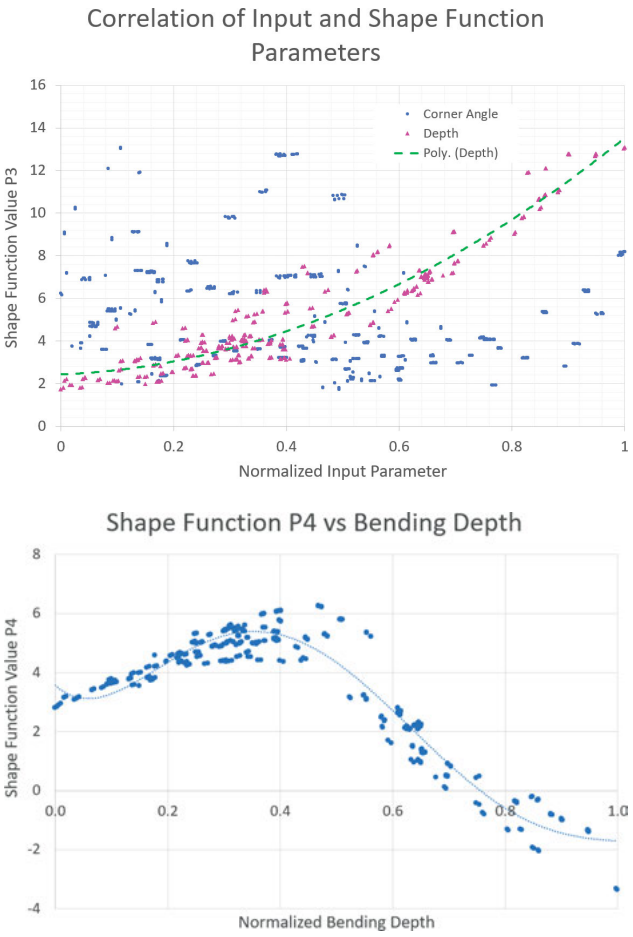

Fig. 8: Correlations of shape parameters relative to normalized inputs.

4.3 Training

With the establishment of the I/O parameters complete (Fig. 9), the process was then executed over 3,500 panels to create the training set. As suggested by the plots in Fig. 9, the relationships between parameters are not linear, so polynomial regression was used. These polynomial regression results can be abstractly represented in 3D visuals, as shown in Fig. 10 and 11. The result of the training is 7 polynomial expressions, one for each sample point, each having the three inputs as the expression variables.

In many ML approaches, the model receives an input database and maps them directly to outputs, with weights and relationships concealed within: the classic "black box" problem. Further, if you query the model with a set of inputs that matches an entry in the database, it may simply return the outputs that were originally paired with

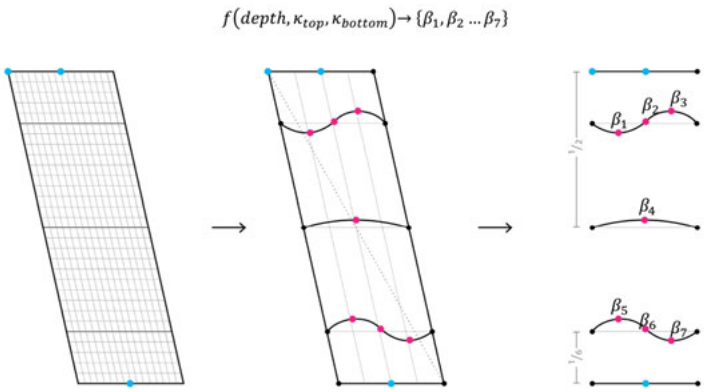

Fig. 9: Function mapping from 3 inputs to 7 output Shape parameters.

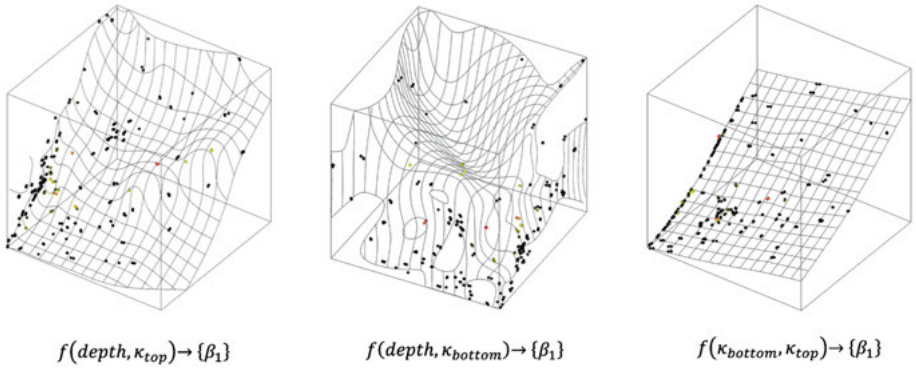

Fig. 10: 3D representations of the ML model, showing two inputs on the horizonal axes, and the resulting shape parameter B1 in vertical.

it. In our case, this is insufficient since the partnered outputs were only approximations. We want to account for the accumulated contours of the sample space, i. e. to "average" across shapes that were similar. By producing a polynomial function, we solve both problems: an explicit description of how the calculation is made, and the function serves as an interpolation of the sample space.

If the predicted 3D surface is found to diverge from the 3D perimeter beyond the agreed tolerance, this indicates there is a gap in the dataset. However, while that simulation was out of tolerance, the deviations were on the order of < 10 mm, meaning the surface was still a decent approximation of the surface's contours. It can therefore be added to the database of approximations, the and model/polynomials retrained. This results in the pseudo-self-improving nature of the ML model.

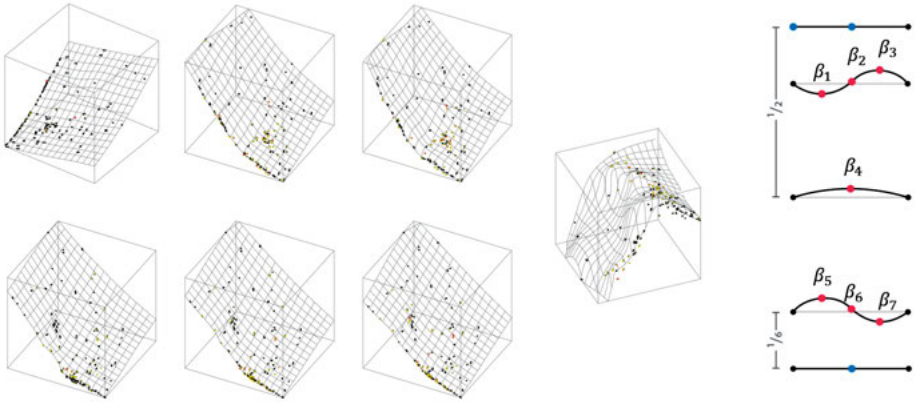

Fig. 11: 3D Representations of all 7 shape functions.

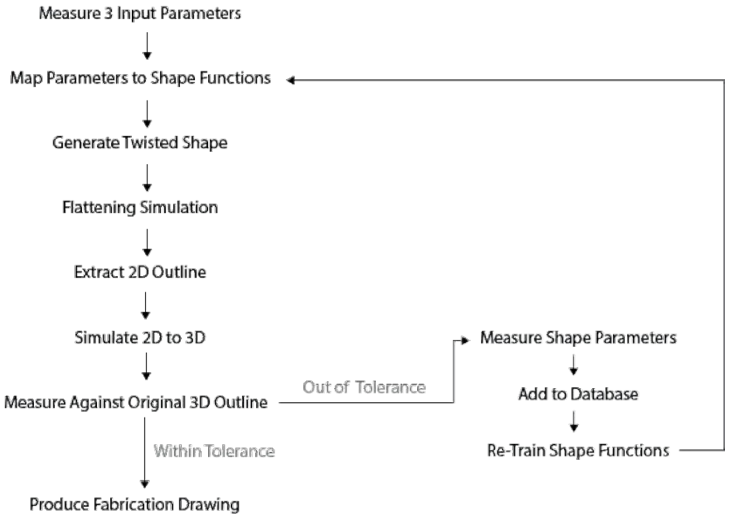

Fig. 12: Flow chart of complete training and production routine.

5 Results and Reflection

By using the ML model to predict the surface geometry of the cold bent, curved, semi-buckled shapes, the edge deviations were reduced from 6.5 mm to a max of 0.5mm, which is well within the allowable threshold. In this regard, the process was useful and constructive. The technique enabled the fabrication of thousands of unique, cold-bend pieces of glass, and to realize the project even with an extremely ambitious timeline.

Fig. 13: Image of some of the unique, highly twisted panels.

We have also shown that current guidance for estimating the buckling threshold appears consistent even with panels that are not rectangular, though the transition is smoother in panels that are skewed.

This study was still centered around a narrow set of geometries and is far from comprehensive. We believe this provides an entry point for a potential larger study across a wider variety of shapes, and the use of ML could provide an efficient way of simulating the "real" surfaces that glass panels will manifest.

The primary motivation for these exercises was fabrication and assembly. However, it would certainly be valuable for architects to be able to assess the aesthetics of surfaces that would arise from given panelizations, a possible extension of this work.

In the context of this building it proved to be critical that any technical solution could fit naturally into a 3D production pipeline. The pace of the project would not have tolerated workflows that require high-friction translations of information across different software packages. While not our central focus, this proved essential for the realities of the project, including time demands and verifiability.

6 Conclusion

As cold bent glazing proliferates as a strategy for realizing complex geometries, one should consider the translation of surfaces represented in CAD environments into reality. Non-planar quadrilaterals are often represented as double-ruled hyperbolic paraboloids. However, we have demonstrated that glass panels appropriate for construction do not adhere to such surfaces, and we present one technique that successfully mapped 3D outlines to a 3-dimensional surface that accounts for material behavior.

Edge deviations were reduced from 6.5 mm to less than 0.5 mm, and the workflow was implemented directly into a 3D CAD production pipeline. Future work should include an expansion of the range of shapes, and a more interactive interface that can be useful for designers.

References

Beer, B. 2015. Structural silicone sealed sold-sent slass–sigh-sise projects experience leading to a new design concept. In *Glass Performance Days 2015 Conference Proceedings,* Tampere, 2015

Bensend, A.: Beneath the surface: buckling of cold formed glass. In: *Glass Performance Days 2015 Conference Proceedings,* Tampere, 2015

Bensend, A. 2016. Maximizing the twist of cold formed glazing. *Challenging Glass Conference Proceedings* 5: 65–80. DOI: 10.7480/cgc.5.2230

Bensend, A. 2018. The Effects of Cold Warping on Glass Stiffness. *Challenging Glass Conference Proceedings* 6: 85–96. DOI: 10.7480/cgc.6.2119

Datsiou, K. C. 2017. Design and Performance of Cold Bent Glass. Thesis, University of Cambridge. DOI: 10.17863/CAM.15628

Datsiou, K. C., and M. Overend. 2016. The Mechanical Response of Cold Bent Monolithic Glass Plates during the Bending Process. *Engineering Structures* 117: 575–90. https://doi.org/10.1016/j.engstruct.2016.03.019.

Eversmann, P., A. Ihde, and C. Louter. 2016. Low Cost Double Curvature – Exploratory Computational Modelling, FE-Analysis and Prototyping of Cold-Bent Glass. *Challenging Glass Conference Proceedings* 5: 81–92. DOI: 10.7480/cgc.5.2233

Galuppi, Laura, Simone Massimiani, and Gianni Royer Carfagni. 2014. Buckling Phenomena in Double Curved Cold-Bent Glass. *International Journal of Non-Linear Mechanics* 64. https://doi.org/10.1016/j.ijnonlinmec.2014.03.015.

Galuppi, Laura, and Gianni Royer Carfagni. 2019. Betti's Analytical Method for the Load Sharing in Double Glazed Units. *Composite Structures* 235: 111765. DOI: 10.1016/j.compstruct.2019.111765

Galuppi, L., G. F. M. Royer-Carfagni, L. Barbieri, and M. Maffeis. 2020. Sharing of general loading in double glazed units. The BAM analytical approach. *Challenging Glass Conference Proceedings* 7. DOI: 10.7480/cgc.7.4484

Gavriil, K., R. Guseinov, J. Pérez, D. Pellis, P. Henderson, F. Rist, H. Pottmann, and B. Bickel. 2020. Computational Design of Cold Bent Glass Facades. *ACM Transactions on Graphics* 39: 1–16. DOI: 10.1145/3414685.3417843

Nardini, V., and J. Hilcken. 2018. Mistral Tower: Value of System Design, Manufacturing and Installation in Cold Bent SSG Units. *Challenging Glass Conference Proceedings* 6: 117–34. DOI: 10.7480/cgc.6.2128